PHYSICAL REVIEW VOLUME 138, NUMBER 5A 31 MAY 1965

Field Control of the Quantum Efficiency of Radiative Recombination in Semiconductors

N. N. Winogradoff*

Advanced Technology Laboratories, IBM Corporation, Federal Systems Division, Washington, D. C.

(Received 30 October 1964; revised manuscript received 20 January 1965)

The bending of the energy bands in a semiconductor by means of a field effect can be used to: (1) reduce the surface recombination velocity, (2) increase the free-carrier concentration in the vicinity of the surface, and (3) reduce the rate of nonradiative recombination through impurity centers. Under suitable conditions which are described, all these factors combine to enhance the quantum efficiency for radiative recombination within the surface-barrier region. A similar situation prevails in the vicinity of a *p-n* junction. The effect of a transverse electric field on the radiative quantum efficiency in Ge, Si, and GaAs is described.

INTRODUCTION

THE quantum efficiency of radiative recombination in semiconductors, defined as the ratio of the rate of production of photons by the recombination of excess carriers to the rate of generation of these carriers, is generally a small fraction. This is mainly due to the presence of other, competitive, nonradiative surface and bulk recombination processes.[1]

The net radiative recombination rate for band-to-band transitions is given by[2,3]

$$R=r(n_0+p_0)\delta_n+\delta_n^2\,, \qquad (1)$$

where n_0 and p_0 are the thermal-equilibrium concentrations of electrons and holes in the semiconductor, respectively, δ_n is the excess concentration of electrons or holes, and r is a constant for a given material and temperature.

The radiative rate can thus be increased by using heavily doped material,[1,3] and we may expect higher quantum efficiencies in such materials. Unfortunately, however, the introduction of high concentrations of dopants introduces crystal imperfections and impurity centers which enhance nonradiative transitions and detract from the quantum efficiency of the radiative process.

On the other hand, the production of accumulation or inversion layers at the surface of a semiconductor by a field effect[4] provides a convenient method of increasing the carrier concentration without the introduction of any additional impurity centers, and as discussed below, can be made to reduce the nonradiative recombination rates through the recombination centers already present in the semiconductor.

Since the field effect can also be used to reduce the surface recombination velocity,[5] it follows that the radiative quantum efficiency can be greatly increased by this technique.

THEORY

The rate of recombination of an excess carrier concentration δ_n, in a semiconductor, may be expressed in terms of an effective lifetime τ_e, such that

$$\tau_e^{-1}=\tau_r^{-1}+\tau_{nr}^{-1}+SL^{-1}\,, \qquad (2)$$

where τ_r and τ_{nr} represent the radiative and nonradiative lifetimes in the bulk of the semiconductor, S is the surface recombination velocity, and L is a constant depending on the dimensions and geometrical configuration of the semiconductor sample and has the dimensions of a length. In general, τ_r, τ_{nr}, and S will all be functions of the excess carrier concentration δ_n.

If the steady-state excess concentration produced by optical injection at the rate g is represented by δ_n, then

$$\delta_n\tau_e^{-1}=g \qquad (3)$$

and Eq. (2) then yields

$$\delta_n/\tau_r=g-\delta_n((1/\tau_{nr})+(S/L)) \qquad (4)$$

as the internal radiative rate. Total internal reflection and internal absorption with and without re-emission, further reduces the intensity of the recombination radiation reaching an external detector to a fraction f of the above radiative rate.

Since the surface recombination velocity S is related to the surface potential ϕ_s, (defined by Fig. 1) by the

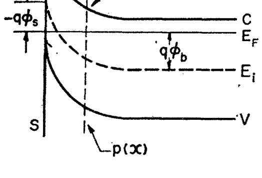

FIG. 1. Schematic diagram defining the surface potential ϕ_s at the surface SS: q is the electronic charge, c the conduction band, v the valence band, E_F the Fermi level, and E_i is an energy level corresponding to the Fermi level of intrinsic material. ϕ_b is the bulk potential.

---

* Present address: National Bureau of Standards, Washington, D. C.

[1] P. T. Landsberg, Proc. Inst. Elec. Engrs. (London), **106B**, 908 (1959).

[2] W. Van Roosbroek and W. Shockley, Phys. Rev. **94**, 1558 (1954).

[3] P. H. Brill and R. F. Shwarz J. Phys. Chem. Solids **8**, 75 (1959).

[4] H. C. Montgomery and W. L. Brown, Phys. Rev. **103**, 865 (1956).

[5] D. T. Stevenson and R. J. Keyes, Physica **20**, 1041 (1954).

expression[6]

$$S=\frac{N_tC_p(p_0+n_0)}{2n_i\exp(q\phi_0/kT)\{\cosh[(E_t-E_i-q\phi_0)/kT]+\cosh[q(\phi_s-\phi_0)/kT]\}}, \tag{5}$$

where C_p is the probability that a hole is captured by a surface state at energy level E_t in unit time, N_t is the density of such states, and $\phi_0=(kT/2q)\ln(C_p/C_n)$, where C_n is the probability of capture of an electron by the state in unit time.

This expression is represented by the bell-shaped curve shown in Fig. 2.

It follows that modulation of ϕ_s by means of an electric field perpendicular to the surface will modulate the surface recombination velocity S in Eq. (4) and that sufficiently high fields yielding values of ϕ_s in the vicinity of points A and B in Fig. 2, will reduce the nonradiative surface recombination rate to negligible values. In this case, Eq. (4) may be rewritten as

$$\delta n/\tau_r=g-(\delta n/\tau_{nr}). \tag{6}$$

The nonradiative bulk recombination process generally implies recombination via trapping centers.[7–9] Denoting the free-electron and hole concentrations at a depth x from the surface of the semiconductor by $n(x)$ and $p(x)$, respectively, the rate of recombination through such centers, at depth x, Fig. 1, is given by[10]:

$$U(x)=\frac{C_nC_p[p(x)n(x)-n_i^2]}{C_n[n(x)+n_1]+C_p[p(x)+p_1]}, \tag{7}$$

where C_n and C_p are the electron and hole capture probabilities for such trapping centers in the bulk, n_i is the intrinsic carrier concentration and n_1, p_1 are the carrier concentrations when the Fermi level coincides with the energy level of the traps.

Since the product $p(x)n(x)$ is independent of x and ϕ_s to the first order of magnitude, and n_1, p_1 are fixed quantities, the recombination rate through these centers is a maximum when $C_nn(x)+C_pp(x)$ is a minimum.

If the excess free-electron and hole concentrations at depth x from the illuminated surface are small compared with the thermal-equilibrium concentrations at that depth, we can write: $n(x)=n_i\exp[E_F-E_i(x)]/kT$ and $p(x)=n_i\exp[E_i(x)-E_F]/kT$, where $E_i(x)$ is the energy of the intrinsic Fermi level at depth x. It follows that the recombination rate is a maximum when

$$E_F-E_i(x)=(kT/2)\ln(C_p/C_n) \tag{7'}$$

or when the "bulk potential" of a section at depth x has the value $(kT/2q)\ln(C_p/C_n)$.

At higher concentrations of excess carrier densities, the quasi-Fermi levels E_{F_n} and E_{F_p} have to be used instead of E_F.

In some cases, recombination through such centers can be radiative,[11] so that the control of the surface recombination velocity by bending bands relative to the Fermi level will influence both nonradiative and radiative recombination rates through impurity centers lying within the depletion or accumulation layers.

Since the surface and bulk recombination centers will, in general, have different energy levels and capture probabilities, their effects on the radiative recombination rate as ϕ_s is swept from, say, positive to negative values, will become apparent at different values of ϕ_s. The change in the recombination rate through the centers located in the bulk of the semiconductor but lying within the depletion or accumulation layers may well account for the apparent increase of the surface recombination velocity at surface potentials to the right and left of points B and A, respectively, in Fig. 2, frequently observed in field-effect measurements.[12]

In general, the nonlinear terms representing the dependence of radiative rates on the concentration of the excess carriers shown in (1) and implied in (7′) renders it difficult to distinguish between radiative transitions taking place directly between the bands and those occurring through recombination centers.

It can be seen, however, that if the excess carrier concentration δ_n in (1) is made to vary sinusoidally as $A\sin^2\pi\nu t$, by suitably modulating the incident beam intensity, (1) may be rewritten as

$$R=r[(n_0+p_0+A)(A/2)(1-\cos 2\pi\nu t)-(A^2/8)(1-\cos 2\pi 2\nu t)]. \tag{8}$$

The photodetector signal thus consists of two components, having modulation frequencies of ν and 2ν, respectively, which can be resolved by passing the signal through a tuned amplifier.

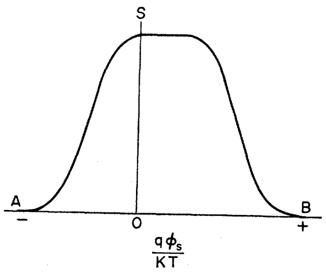

FIG. 2. Curve showing the dependence of the surface recombination velocity S on the surface potential ϕ_s.

---

[6] T. B. Watkins, *Progress in Semiconductors* (John Wiley & Sons, Inc., New York, 1960), Vol. **5**, p. 1.

[7] R. N. Hall, Proc. Inst. Elec. Engrs. (London) **106B**, 923 (1959).

[8] G. Bemski, Proc. IRE **46**, 990 (1958).

[9] A. R. Beatti and P. T. Landsberg, Proc. Phys. Soc. (London) **249**, 61 (1959).

[10] W. Shockley and W. T. Read, Phys. Rev. **87**, 835 (1952).

[11] J. R. Haynes and W. C. Westphal, Phys. Rev. **101**, 1676 (1956).

[12] P. Balk (private communication).

The ratio of the two signals, represented by R_ν and $R_{2\nu}$ is given by

$$R_\nu/R_{2\nu}=4(n_0+p_0+A)/A\,. \tag{9}$$

If $A\gg n_0+p_0$, this ratio tends to a limit of 4. In the steady state, equality of the rates of generation and recombination yield: $A=\delta n=\alpha I\tau_e$, where α is the absorption coefficient, I is the intensity of the incident radiation, and τ_e is the effective lifetime of the excess free carriers.

With high-resistivity Si, less than a microwatt of radiation at 2.0 eV should suffice to yield a ratio of 4.5.

The main advantage of applying this technique to the detection of band-to-band recombination lies in the fact that the amplitude of the 2ν signal is uniquely proportional to the square of the incident light intensity.

The multiplying action implied in expressions (1), (8), and (11) provide an interesting possibility of further enhancing radiative-recombination rates by optical or electrical pumping. Suppose that a wafer of a semiconductor is illuminated by two independent beams of highly absorbed light, resulting in excess carrier densities δn_1 and δn_2, respectively. Expression (1) then expands into

$$R=r[(n_0+\delta n_1+\delta n_2)(p_0+\delta n_1+\delta n_2)]-rn_0p_0\,. \tag{10}$$

If now one of the beams is modulated so that δn_1 varies sinusoidally as $A\sin^2\pi\nu t$, as before, while the other beam is kept constant, we again obtain signals modulated at frequencies ν and 2ν which can be resolved by means of a tuned amplifier. The amplitude of the ν signal is given by

$$R_\nu=r(n_0+p_0+A+2\delta n_2)A/2\,. \tag{11}$$

Denoting this amplitude as $R_{\nu p}$ when $\delta n_2\neq 0$ and by R_ν when $\delta n_2=0$, the ratio of the signals at the incoming signal frequency ν with and without the local incoherent light pump source p, is given by

$$R\nu_p/R_\nu=1+2\delta n_2/(n_0+p_0+A)\,. \tag{12}$$

If $A\ll n_0+p_0$ and $\delta n_2\gg n_0+p_0$, considerable enhancement of the recombination radiation should take place at the frequency ν of the incident signal and actual amplification of incoherent light appears to be possible.

Experimental verification of the control of the quantum efficiency of radiative recombination by means of a field effect, and confirmation of the effects described above are presented below and used for the identification of the radiative mechanism.

EXPERIMENTAL PROCEDURE

Since the above effects, related to the modulation of the surface potential ϕ_s, were restricted to regions of the semiconductor close to the surface, the carrier generation was produced by optical injection by illuminating the appropriate surface with light characterized by a high absorption coefficient.

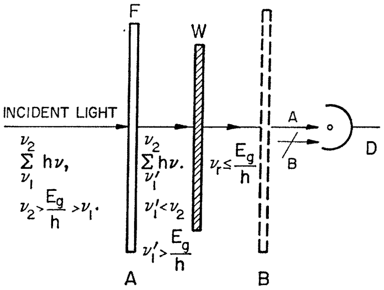

FIG. 3. Schematic diagram illustrating the filter characteristics and experimental arrangement. F is a low-cut filter which can be in one of two positions A or B relative to the semiconductor wafer W and detector D.

Direct transmission of incident light through the semiconductor was prevented by the use of appropriate long-wavelength cutoff filters, and the identification of the radiation emerging from the back surface (of a front illuminated semiconductor wafer) with recombination radiation was checked by comparing the intensity of the radiation reaching the detector D (Fig. 3) when the filters were placed in front of the wafer (position A) and behind the wafer (position B), Fig. 3.

The intensity of the transmitted light would be unaffected by a change in position of the filters, while position B would prevent recombination radiation from reaching the detector.

Typically, a few centimeters of water sufficed to cut off transmission with Ge wafers while 4-mm KG 3 Schott glass filters[13] sufficed in the case of Si wafers, and 3 mm of BG 18 Schott glass was satisfactory in the case of GaAs. The wafer thicknesses used ranged from 0.3 to 1.0 mm.

Photomultipliers with $S1$ spectral response were used to detect the recombination radiation emitted by Si and GaAs, and a sensitive PbS detector measuring 1.5×2 cm placed very close to the back surface of the wafer was used for the detection of the recombination radiation from Ge.

Improved signal-to-noise characteristics were obtained by chopping the incident visible light, and by using a tuned amplifier to detect the recombination radiation signal. This technique permitted the ac light signal to be distinguished from any electrical injection

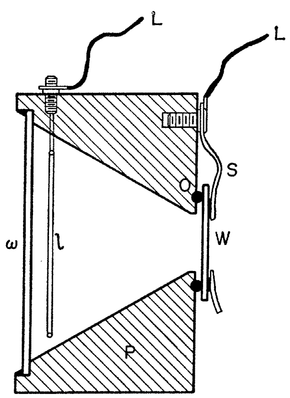

FIG. 4. Schematic drawing of the electrolytic cell consisting of a plastic body P, optical window w, spring contact S holding a semiconductor wafer W against a rubber O ring 0, and fitted with a platinum-loop electrode and leads L.

---

[13] Jenaer Glaswerk Schott & Gen, Mainz, West Germany.

luminescence produced by the applied voltage. By using a low-frequency sinusoidal chopper consisting of a polaroid disc rotating in front of a fixed sheet of polaroid, the light intensity could be modulated sinusoidally while the area of the semiconductor under illumination remained constant.

Since large changes in the surface potential ϕ_s could be obtained by applying small potential differences across a semiconductor-electrolyte interface,[14] this method of providing a field effect was preferred to the "dry"-field-effect system requiring high voltages.

An opaque plastic cell with a conical cavity served as an electrolytic cell. The wide opening was closed with a suitable optical window as shown in Fig. 4. The smaller opening of the cavity was closed by pressing the semiconductor wafer against a soft rubber O ring surrounding this opening, by means of a spring contact, bearing against an ohmic ring contact on the back surface of the semiconductor.

The central clear portion of this ring contact together with a hole in the above spring, permitted the recombination radiation to reach the detector.

The modulating field across the semiconductor-electrolyte interface was obtained by connecting a voltage source across the above spring contact and an inert platinum loop electrode dipping into the electrolyte. Under these conditions, a change of potential of less than 2 V sufficed to change the intensity of the recombination radiation by more than an order of magnitude. A schematic drawing of the optical system and electronic display arrangement permitting the intensity of the recombination radiation or photocurrent to be plotted against the applied voltage is shown in Fig. 5.

EXPERIMENTAL RESULTS

(a) Control of Surface Recombination Effects

Inspection of Eq. (4) and the bell-shaped curve representing the variation of the surface recombination velocity with the surface potential ϕ_s would be expected to yield an inverted bell-shaped curve representing the variation of the radiative recombination rate with surface potential as shown by the dotted line in Fig. 6, the minimum of the radiative rate coinciding with the maximum value of the surface recombination velocity S.

As shown in Fig. 6, the curve representing the variation of the radiative recombination rate with a change in surface potential obtained with a 57 Ω-cm *p*-type silicon wafer, characterized by a lifetime τ_e of 400 μsec, confirms the general inverted bell shape expected. By using wafers of different conductivity types the position of the minimum shifted along the voltage axis as expected from theory,[5] but the actual magnitude and sign of the field across the interface depended on the applied potential difference and on the internal emf of the Si/H_2SO_4–H_2O/Pt system which in turn depended on the state of polarization of the electrodes. Since this was difficult to measure and was of little significance to the present investigation, the surface potential ϕ_s was represented by the voltage observed between the platinum electrode and the back contact on the semiconductor wafer. As the applied voltage was swept from a negative to a positive potential difference, the radiative recombination rate was observed to go through a minimum as expected, as shown in Fig. 6.

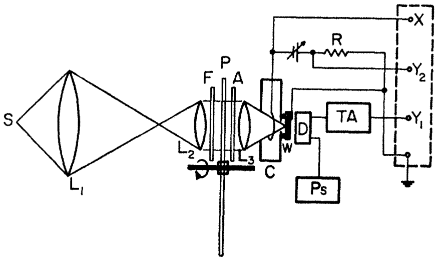

FIG. 5. Schematic drawing of the apparatus used. S-Light source (filament or mercury-vapor bulb), L_1, L_2, L_3 are lenses, F is a filter, P is a rotating polaroid analyzer, C is the electrolytic cell, W is a semiconductor wafer, D is a detector, P_s is the power supply for the detector, TA is a tuned amplifier, and R is a dropping resistor for measuring the photocurrent. X, Y_1, Y_2 are the inputs to a display or recording system. *Note*: In general, the effect of slow surface states yielded serious drifts in the signal amplitude at a given bias. For this reason all the curves presented were derived from cathode-ray or X-Y recorder traces generated by the light signal while the biasing voltage was swept mechanically at a uniform rate of about 5 sec per volt.

Although expressions (4) and (5) would be expected to result in a R versus ϕ_s curve with symmetry about the minimum, the experimental curves show a lack of symmetry in the slopes dR/dv, and in the saturation values of R on both sides of the minima, but the general inverted bell shape of the curve can be clearly seen.

The difference in the slopes on the two sides of the minima is due to a nonlinear characteristic of ϕ_s versus

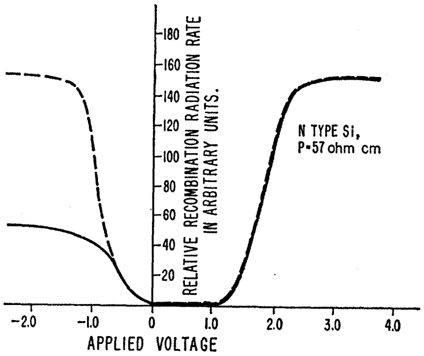

FIG. 6. Curve showing dependence of radiative-recombination rate on the applied voltage. The polarity of the voltage indicated was that on the semiconducting wafer. Qualitatively similar results were obtained with a wide range of resistivities and with Ge samples.

---

[14] H. U. Harten, Proc. Inst. Elec. Engrs. (London) **106B**, 906 (1959).

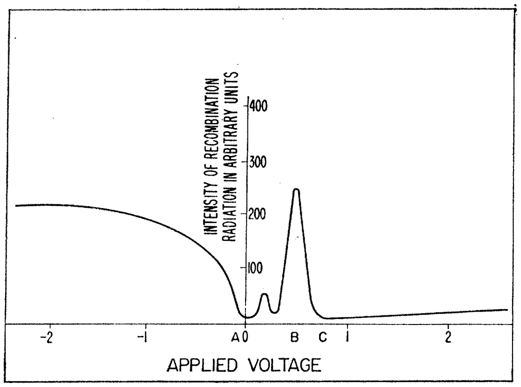

FIG. 7. Curve showing successive enhancement and quenching of radiative recombination as various recombination centers pass through the optimum energies relative to the Fermi level.

applied voltage, while the difference in the saturation levels of the radiative rates R may be attributed to a change in lifetime of the material due to a shift of the Fermi level relative to the recombination center[10,15] as discussed above, and particularly well illustrated by some Ge samples, a typical curve for which is shown in Fig. 7.

(b) Nature of the Radiative Recombination Mechanism

With the exception of one sample of high purity intrinsic Ge with a very low dislocation count, no 2ν signal expected from Eq. (8) was observed with wafers of Ge, Si, and GaAs covering a wide range of resistivities (0.7–55 Ω-cm for Ge, 0.1–11×10^3 Ω-cm for Si, and 10^{-2}–10^{-4} Ω-cm for GaAs).

The amplitude of the ν signal observed with the Si wafers was almost proportional to the square of the intensity of the incident light. In terms of expression (14) this would imply that $A \gg (n_0+p_0)$ in these samples, and we should have been able to see a signal at frequency 2ν. Failure to do so except in one clear-cut case of high-purity Ge, is taken to indicate that the band-to-band recombination of free carriers in all the samples tested produced a negligible contribution to the recombination radiation emitted by these samples, and that the radiative process implied transitions through radiative-recombination centers. We shall return to some aspects of these centers in the discussion below.

(c) The Behavior of Radiative- and Nonradiative-Recombination Centers in a Surface Barrier Produced by a Field Effect

We have already discussed the dependence of radiative and nonradiative carrier transition rates through the recombination centers in terms of the energy difference between the actual and intrinsic Fermi levels. It follows that as the surface potential ϕ_s is swept over a sufficient range, the various types of centers in the surface-barrier region will pass through energy values which will yield maxima in radiative or nonradiative transition rates through the appropriate center.

The intensity of the recombination radiation emitted by the wafer would thus go through a series of maxima and minima as shown in Fig. 7 representing curves frequently observed with Ge samples.

The minimum A in the radiative rate at low applied fields is attributed to a maximum in surface recombination velocity, the maximum in the radiative rate in the region B is attributed to an enhanced radiative rate as the energy difference between the actual and intrinsic Fermi levels E_F-E_i tends toward the optimum value of $(kT/2)\ln(C_p/C_n)$ as discussed above. This enhancement is first partially and then fully compensated by a similar increasing rate of nonradiative recombination through another set of centers with a somewhat broader distribution of energy levels, resulting in a minimum in the radiative rate at voltage C.

Further and clearer evidence for a maximum in radiative recombination rate as the energy difference E_F-E_i goes through the critical value of $(kT/2)\ln(C_p/C_n)$ was obtained with a sample of degenerate p-type GaAs (Zn doped to 7.5×10^{18} cm^{-3}) shown in Fig. 8.

In common with all other GaAs wafers tested, little or no surface recombination effects were observed.

(d) Enhancement of Modulated Radiative Recombination by Optical Pumping

The enhancement of the radiative recombination signal modulated with the chopping frequency ν, by the simultaneous illumination of the surface of the semiconductor by another steady light (pump) source, predicted by Eq. (7) derived above, was observed with Ge and Si samples.

Typical results obtained with Si wafers are illustrated in Fig. 9 and clearly show that even with moderate pump sources, enhancements of more than two orders of magnitude were easily obtained.

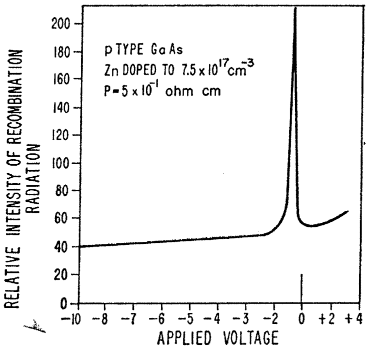

FIG. 8. Curve showing variation of photoluminescence in GaAs with biasing voltage.

---

[15] A. Rose, *Concepts in Photoconductivity* (Interscience Publishers, Inc., 1963), p. 24.

DISCUSSION OF RESULTS

The results presented above suggest that the main radiative process in the samples investigated took place via a radiative recombination center. The radiative rate should therefore be represented by an equation of the form: $R=BNp$, where B is a constant, N is the concentration of traps in a state capable of radiating by the capture of a carrier, and p is the concentration of such free carriers.

If p is made to vary sinusoidally as described above, the amplitude of the intensity of the recombination radiation at the chopping frequency ν should be proportional to A. This proportionality was observed with GaAs and to a lesser extent with Ge, where the radiative rate was slightly supralinear for all light levels used. On the other hand, in Si, the amplitude of this signal was found to be proportional to A^2, i.e., the square of the incident light intensity. It thus appears that N, the concentration of radiative recombination centers is itself proportional to the intensity of the incident light. This may result from the trapping of a free carrier by such a center or the center may be triggered into the appropriate state for radiative capture by the emptying of a filled center by the incident light. The situation in the latter case corresponds to the photoconductive mechanism proposed for CdS.[16]

Both models yield a situation which is identical to that used in discussing charge-extraction effects in CdS surface barriers.[17] Since charge extraction results in current flow, the correlation of the radiative recombination rate and photocurrent generated by the incident light was examined by the simultaneous display of both these characteristics as a function of the applied voltage. The result obtained with a 78 Ω-cm p-type Si wafer is shown in Fig. 10.

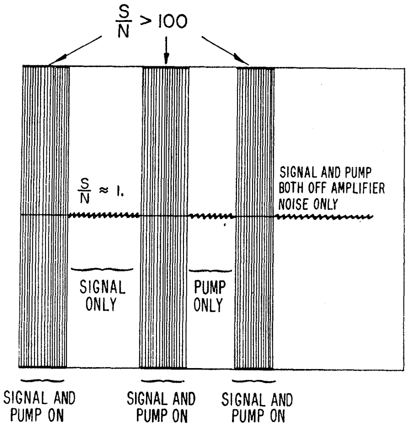

FIG. 9. A reproduction of a cathode-ray display of the signal from a photomultiplier receiving the recombination radiation generated in p-type 63-ohm-cm Si under the stated conditions of illumination. The shaded areas represent the resolution of individual cycles of the 40-cps chopper in the signal beam with a slow cathode-ray traverse rate.

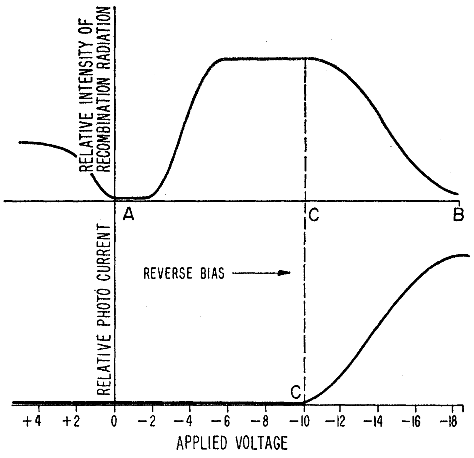

FIG. 10. Curve showing correlation of the variation of the intensity of photoluminescence (top curve) and photocurrent (bottom curve) with applied biasing voltage.

Since the quenching of the radiative rates at low and high *reverse* (p-type Si negative) biases is associated with zero and maximum current flow, respectively, the quenching mechanisms in the two cases must be different. The low-voltage minimum at A is attributed to surface recombination processes as discussed above.

The coincidence of the onset and saturation of the photocurrent with the decline and disappearance of radiative recombination at C and B, respectively, in Fig. 10 may also be explained by the shift of the energy level of the recombination center relative to the Fermi level within the depth of penetration of the incident light as shown in Fig. 11.

By virtue of the bending of the bands by the applied-field-effect voltage, the bulk semiconductor may be subdivided into two regions: one, closest to the surface, where the energy level of the recombination centers (assumed to be donor type) are more than $kT\ln(C_p/C_n)$ below the Fermi level and therefore filled with electrons, and the other where their energy level is less than $kT\ln(C_p/C_n)$ below the Fermi level. With increasing bias the former region will penetrate deeper into the wafer.

If the depth of penetration of the incident light is less than the thickness of the first region, free carriers

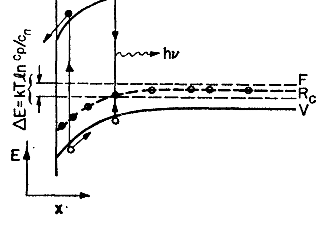

FIG. 11. Schematic diagram illustrating the position of optimum radiative recombination in a surface barrier.

---

[16] N. N. Winogradoff, Appl. Phys., 32, 506 (1961).

[17] P. J. Daniel, R. F. Schwartz, M. E. Lasser, and L. W. Hershinger, Phys. Rev. 111, 1240 (1958).

produced by the incident light will be swept apart by the junction field. The holes will be driven towards the second region where hole capture will be negligible.[18] Similarly the free electrons will be driven toward the surface into regions where electron capture is negligible.

Under these circumstances, there will be no carrier flow through the recombination centers and the free carriers will contribute to a flow of current with negligible light emission, a situation which is represented by applied voltages in excess of B. The corresponding saturated photocurrent in this voltage range represented a quantum efficiency of 0.93.

As the applied voltage is decreased, the first region discussed above shrinks and the second region expands into the region where free carriers are being produced by the incident light. Under those conditions, the surface-barrier field is weaker and electrons are readily captured by the recombination centers now predominantly filled with holes. The electron capture is radiative and a hole is then captured to return the center to its steady-state condition. This process thus yields light emission at the expense of a photocurrent.

Further enhancement of the radiative rate is produced by the movement of the region where the energy level of the recombination center is $kT \ln(C_p/C_n)$ below the Fermi level toward the surface into regions where the intensity of the incident radiation, and therefore the free-carrier generation rate is higher, as the applied voltage is reduced.

In the limiting case, as the bands are straightened, surface recombination removes the carriers before they can recombine radiatively through the centers.

Under forward bias, the second region spreads throughout the thickness of the wafer. The surface-barrier field now drives the electrons away from the surface into the p-type material where they will recombine both radiatively and nonradiatively and little photocurrent will flow. A more rigorous treatment of the effects must necessarily include the quasi-Fermi level concept but the basic argument remains unchanged.

CONCLUSIONS

The experimental results described above clearly illustrate the possibility of controlling the quantum efficiency of radiative recombination by means of a field effect.

The results indicate that free-carrier band-to-band radiative recombination plays a negligible role in the photoluminescence of Ge, Si, and GaAs, and that the main radiative process takes place through a recombination center.

The control of radiative efficiency is brought about by varying the nonradiative surface and bulk recombination rates by varying the position of the energy levels of the various recombination centers relative to the Fermi level, in the region where free carriers are generated. Detailed analysis of the results suggests that the same center may give rise to radiative or nonradiative recombination.

Since the difference in energy E_F-E_i, between the actual and intrinsic Fermi levels, will vary across the depletion region of a p-n junction, the origin of the light emitted by a forward biased junction will be determined by the region where this energy difference reaches an optimum value of $(kT/2)\ln(C_p/C_n)$, and this may move with the applied bias. In some cases, the nonradiative recombination centers to the n-type side of the radiative center may be in a more favorable state for recombination flow; if these cannot be eliminated, the nonradiative recombination through these centers can be reduced by a reduction of the volume of the space-charge region favoring the critical energy relationship for E_F-E_i. This may be accomplished by using a partially abrupt junction and appears to be of importance in semiconductor lasers.[19]

Considerable enhancement of the modulated component of recombination radiation produced by a weak modulated light beam can be produced by simultaneously illuminating the semiconductor with another intense steady "pumping" light beam.

ACKNOWLEDGMENTS

The author would like to thank Dr. G. R. Gunther-Mohr for many helpful discussions and his encouragement in this work, Dr. O. T. Anderson and J. J. Leybourne for considerable help in the critical experiments, H. K. Kessler for advice and assistance in the instrumentation used, and G. Harman of the National Bureau of Standards for further helpful discussions.

---

[18] J. S. Blakemore, *Semiconductor Statistics* (Pergamon Press, Inc., New York, 1962), p. 261.

[19] N. Winogradoff and H. K. Kessler, Solid State Commun. **2**, 119 (1964).